

## Plasma-screening effects on electron-impact excitation of hydrogenic ions in dense plasmas

B. L. Whitten\* and N. F. Lane

*Physics Department and Rice Quantum Institute, Rice University, Houston, Texas 77251*

J. C. Weisheit\*

*Plasma Physics Laboratory, Princeton University, Princeton, New Jersey 08540*

(Received 8 February 1982; revised receipt date 19 October 1983)

Debye-Hückel and ion-sphere plasma screening models have been used in a study of inelastic scattering of electrons by one-electron ions in dense, high-temperature plasmas. Cross sections for transitions among the  $1s$ ,  $2s$ , and  $2p$  states have been calculated using close-coupling and distorted-wave descriptions. The optically allowed  $1s \rightarrow 2p$  and  $2s \rightarrow 2p$  cross sections are substantially reduced at all energies by plasma screening of the long-range dipole coupling. The  $1s \rightarrow 2s$  cross section is less sensitive to plasma effects. For an ion of nuclear charge  $Z$ , the scaled inelastic cross sections  $Z^4 Q$  are roughly independent of  $Z$  for fixed values of  $E/Z^2$  and  $Z\Lambda$  or  $ZR_z$ , where  $E$  is the electron's kinetic energy,  $\Lambda$  is the Debye length, and  $R_z$  is the ion-sphere radius.

### I. INTRODUCTION

In the last decade or so, interest in the properties of hot, dense plasmas has grown, in part because of applications to the design of inertial confinement fusion targets and the search for short wavelength lasers. In both of these cases, the plasma is sufficiently short-lived that it cannot come to equilibrium, and detailed understanding of the rates of various processes is required for an adequate description of the plasma. In particular, in dense, high-temperature inertial confinement plasmas, the determination of particle densities and temperatures from spectral line emission requires knowledge of the spectroscopic and collision properties of ions under extreme conditions.<sup>1-3</sup> In such experiments, ion densities of  $10^{21}$ – $10^{23}$  cm<sup>-3</sup> and plasma temperatures of  $10^7$  K are typical; higher densities and temperatures are anticipated for experiments in the near future.

Under these conditions, the plasma environment can be expected to significantly influence many atomic processes, primarily through the screening of long-range electrostatic interactions by charged particles. Some recent progress has been made in estimating the influence of the plasma on atomic structure,<sup>4,5</sup> and on various radiative processes<sup>6</sup>; however, information on scattering processes is very limited. A study<sup>7</sup> of inelastic electron collisions with one-electron ions, using the (nonunitarized) Born I approximation for the collision dynamics, showed that inelastic cross sections are significantly reduced by Debye-Hückel screening of the electron-ion interaction. However, the Born approximation can be expected to fail near threshold, where distortion effects can be large. For many transitions, namely those in which the mean kinetic energy of plasma electrons is well below excitation threshold, it is the near-threshold region that is most important.

In this paper, we examine the effects of plasma screening on electron-impact excitation cross sections for  $1s \rightarrow 2s, 2p$  and  $2s \rightarrow 2p$  transitions of hydrogenic ions of

nuclear charge  $2 \leq Z \leq 18$ . We study the underlying dynamics of the collision by comparing results from the Born I, distorted-wave, and few-state close-coupling models. We also explore the dependence of the cross sections on the description of plasma screening by comparing results for the Debye-Hückel and ion-sphere potentials.

We wish to emphasize that treatment of a plasma's influence on collision events by means of a model potential results from the approximation in which the net electrostatic interaction due to the specific configuration of background particles existing at the time of the collision is replaced by the average net interaction of an appropriate distribution of configurations. This approximation might be expected to be accurate when the collision duration is much larger than the characteristic plasma response time (i.e., the reciprocal of the plasma frequency) and/or when fluctuations about the average interaction are small. Without this simplification, cross sections must be computed as functions of both the net plasma microfield  $\vec{F}$  and the relative momentum  $\hbar\vec{k}$ , and then an appropriate average taken with respect to the field strength distribution and the angle between  $\vec{F}$  and  $\vec{k}$ . An investigation of some scattering problems within this framework would be very worthwhile, but is beyond the scope of the present study.

### II. PLASMA INTERACTION

In a dense, hot plasma, both thermal and Coulomb effects must be considered. The relative importance of these two can be estimated by the so-called Coulomb parameter  $\Gamma \equiv \langle Z_i e \rangle^2 / R_i kT$ , where  $\langle Z_i e \rangle$  is the average charge of ions in the plasma, and  $R_i$  is the average interionic distance.<sup>3</sup> In the limits where one or the other effect dominates, one can derive a simple analytic potential to describe the plasma screening of the charged particles.

In the high-temperature, low-density limit ( $\Gamma \ll 1$ ), linearization of the Poisson-Boltzmann equation leads to

the Debye-Hückel potential.<sup>8</sup> This is a particularly appropriate choice for a scattering problem, since Stewart and Pyatt<sup>9</sup> have shown that the potential of an ion in a plasma approaches the Debye-Hückel potential far from the ion. Also, Rozsnyai<sup>10</sup> has found that the Debye-Hückel model is a good approximation of the Hartree-Slater potential at large distances from an ion in a hot plasma.

In the low-temperature, high-density limit, where Coulomb effects are dominant ( $\Gamma \gg 1$ ), the ion-sphere potential is a reasonable approximation. Here it is assumed that the positive ions are fixed, and that each ion is surrounded by a sphere of radius  $R_z$  (the ion-sphere radius), containing  $Z$  uniformly distributed electrons.<sup>8</sup>

Both of these model potentials are appropriate to the problem of a bare nucleus in a plasma. Since we are interested in one-electron ions, we must also describe the interaction between the bound and projectile electrons. In this study we have chosen the simplest approach, namely, to screen this interaction using the same spherical screening factor as that derived for the projectile electron-nucleus interaction. Thus, for the case of Debye-Hückel screening we approximate the electron-ion interaction energy by

$$V(\vec{r}_1, \vec{r}_2) = \left[ -\frac{Z}{r_1} + \frac{1}{r_{12}} \right] \exp(-r_1/\Lambda), \quad (1)$$

where

$$\Lambda \equiv \left[ 4\pi e^2 \frac{N_e}{kT} \right]^{-1/2} \quad (2)$$

is the Debye length;  $\vec{r}_1$  and  $\vec{r}_2$  represent the coordinates of the projectile and bound electrons, respectively;  $Z$  is the nuclear charge,  $N_e$  is the electron density in the plasma, and  $T$  is the electron temperature. We have included only the plasma electrons in the definition of  $\Lambda$  because the target ion is presumed to possess kinetic energy approximately equal to the mean ion energy, and therefore cannot be efficiently screened by other plasma ions.<sup>11</sup>

Analogously, we define the ion-sphere potential as

$$V(r_1, r_2) = \begin{cases} \left[ -\frac{Z}{r_1} + \frac{1}{r_{12}} \right] \left[ 1 - \frac{r_1}{2R_z} \left( 3 - \frac{r_1^2}{R_z^2} \right) \right], & r \leq R_z \\ 0, & r > R_z. \end{cases} \quad (3)$$

In Eq. (3)  $\vec{r}_1$ ,  $\vec{r}_2$ , and  $Z$  are defined as before, and the ion-

sphere radius is

$$R_z \equiv \left[ \frac{3(Z-1)}{4\pi N_e} \right]^{1/3}. \quad (4)$$

These choices are somewhat arbitrary. However, we can partially justify the assumption of spherically symmetric screening by noting that the rapid periodic motion of the bound electron will tend to average its interaction with plasma electrons. Limited experimentation with other descriptions of the electron-electron interaction<sup>7</sup> suggests that this choice, which strongly screens all matrix elements, maximizes the plasma's effect on the cross section. Table I contains a list of the relevant plasma parameters for all calculations we will discuss; the parameters represent typical dense plasma conditions.

### III. COLLISION DYNAMICS

We calculated the excitation cross sections using the few-state close-coupling method. The formulation of the collision problem is identical to that of electron-hydrogen scattering<sup>14,15</sup> in which exchange is ignored. The rationale for ignoring exchange effects is simply that, for the larger partial-wave angular momenta where plasma screening is expected to be important, exchange effects in the excitation of unscreened target ions are small. This point will be discussed in more detail in Sec. V.

The cross section for  $n, l_a \rightarrow n', l'_a$  excitation of one-electron ions induced by a collision with an incident electron having kinetic energy  $\frac{1}{2}k^2$  (atomic units are used throughout) is<sup>14</sup>

$$Q(nl_a \rightarrow n'l'_a) = \frac{\pi}{(2l_a + 1)k^2} \sum_{L=0}^{\infty} \Omega_L(nl_a, n'l'_a). \quad (5)$$

The partial collision strength  $\Omega_L$ , symmetric in target-state quantum numbers, is defined in terms of the  $T$  matrix elements by

$$\Omega_L(nl_a, n'l'_a) = (2L + 1) \sum_{l''} |T(nl_a l, n'l'_a l'')|^2, \quad (6)$$

where  $|l_a - l| \leq L \leq l_a + l$ ,  $|l'_a - l'| \leq L \leq l'_a + l'$ , and where  $l_a$ ,  $l$ , and  $L$  are the angular momentum quantum numbers for the bound electron, projectile electron, and the total system, respectively.

For this problem, we assign charge  $Z$  to the nucleus,

TABLE I. Plasma parameters for scattering calculations.

Ion	$Z$	$kT$ (eV)	$N_e$ (cm <sup>-3</sup> )	$\Gamma$	$\Lambda(a_0)$	$R_z(a_0)$
He <sup>+</sup>	2	4	7.86 (20) <sup>a</sup>	0.535	10.0	12.7
			3.52 (20)	0.410	15.0	16.6
			5.96 (19)	0.226	36.4	30.0
Ne <sup>9+</sup>	10	500	1.09 (24)	0.430	3.0	2.37
			6.71 (22)	0.170	12.1	6.00
Ar <sup>17+</sup>	18	1000	7.06 (24)	0.757	1.67	1.57
			7.69 (23)	0.361	5.06	3.33

<sup>a</sup>Numbers in parentheses represent the powers of 10 by which the entries must be multiplied.

and screen all matrix elements as described in Sec. II. The intra-atomic Coulomb potential is not screened; the bound-state wave functions are taken to be hydrogenic. This approximation should be good for low-lying bound states, since these compact wave functions should feel little plasma screening. (This is evidenced by the small plasma polarization shifts measured for resonance transitions involving low-lying excited states.<sup>16</sup>) The coupled radial equations are integrated using the Green's-function technique.<sup>17</sup> In order to examine some aspects of the collision dynamics, we also obtained the Born I and distorted-wave cross sections by ignoring certain matrix elements in the coupled equations.

The Born I approximation (BI) is a weak-coupling approximation based on plane-wave scattering states. It ignores flux "feedback" from final to initial channels, and

takes no account of the effect of the large nuclear attraction on the scattered electron's trajectory (i.e., the distortion of the free electron wave). BI is valid at high energies, or for large- $l$  (hence, in this case, large- $L$ ) partial waves at all energies. The Coulomb-Born approximation (CBI) is identical with BI except the plane waves are replaced by Coulomb waves.<sup>18</sup> Since in the plasma all long-range interactions are screened, CBI is not really appropriate; however, it will provide us with one means of comparing our screened results with bare-ion calculations. (The notations BI and CBI are used to distinguish these from the alternative, "unitarized" versions BII and CBII.<sup>14</sup>)

The distorted-wave approximation (DW) is also a weak-coupling approximation, but diagonal matrix elements are retained in the coupled equations so that distortion of the incident and scattered electron waves by the

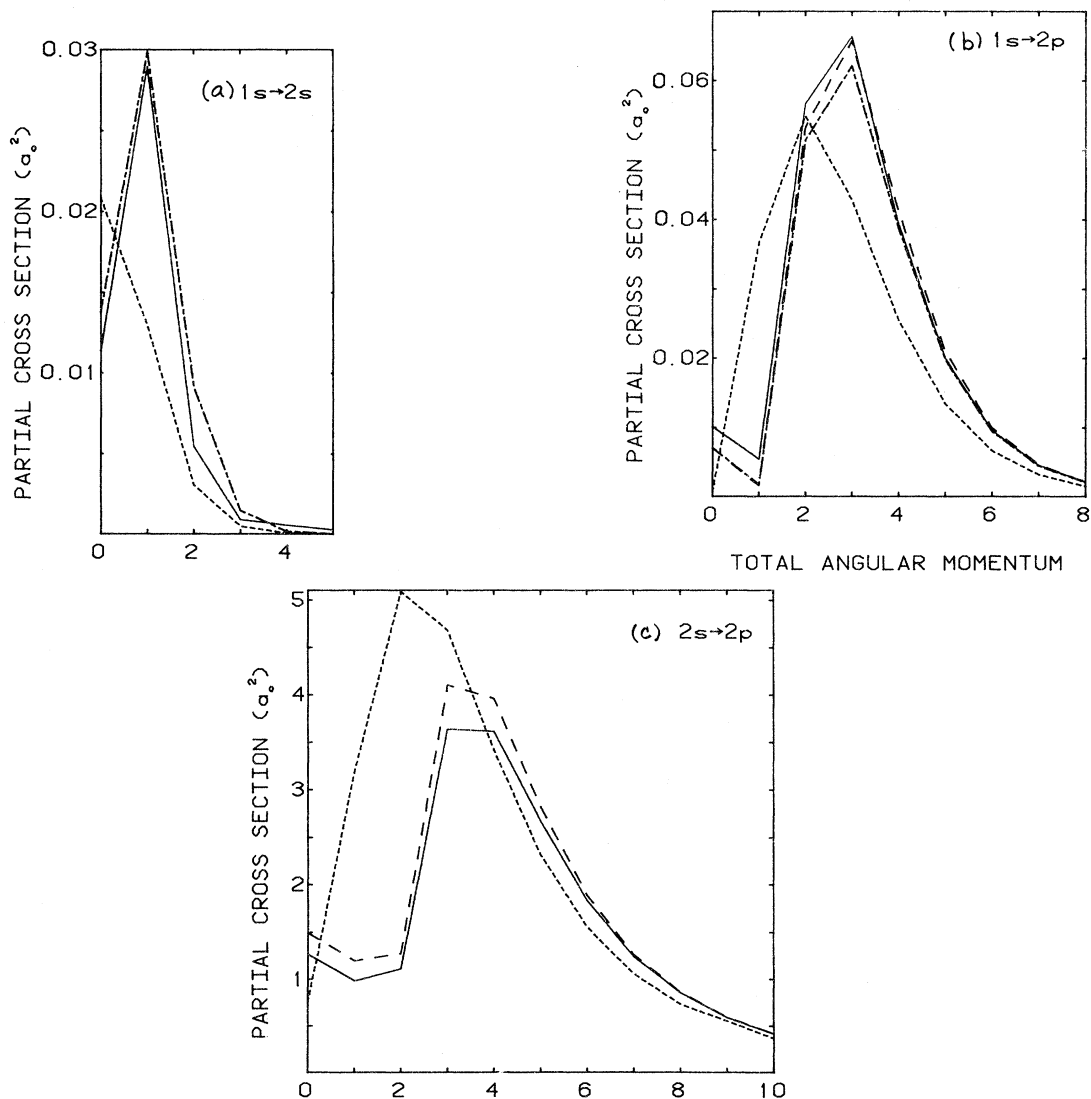


FIG. 1. Partial excitation cross sections versus total angular momentum for  $e\text{-He}^+$  scattering. Plasma represented by Debye-Hückel model with  $\Lambda = 10a_0$  (5.29 Å). Solid line (3 CC); dotted-dashed line (2 CC); dashed line (DWII); dotted line (BI). (a)  $1s$  to  $2s$  cross section. Energy = 81.6 eV (twice threshold) (2 CC and DWII results are the same). (b)  $1s$  to  $2p$  cross section. Energy = 81.6 eV (twice threshold). (c)  $2s$  to  $2p$  cross section. Energy = 13.6 eV (3 CC and 2 CC results are the same).

average field of the ion is included. We denote the distorted-wave results DWII since a symmetric distorted-wave  $K$  matrix is assumed so that the resulting  $S$  matrix is unitary (this is analogous to Seaton's unitarized Born II approximation).

#### IV. RESULTS

##### A. Distortion and coupling effects

We calculated partial and total cross sections for the  $1s \rightarrow 2s$ ,  $1s \rightarrow 2p$ , and  $2s \rightarrow 2p$  transitions in  $e\text{-He}^+$  collisions, using the Born I (BI), distorted-wave (DWII), and two- and three-state close-coupling methods (2 CC, 3 CC). The plasma-screening model used here is the Debye-Hückel approximation leading to the interaction potential

energy of Eq. (1). For purposes of illustration we used the Debye-Hückel interaction of Eq. (1) and chose a Debye length of  $10a_0$  ( $5.29 \text{ \AA}$ ); for a 4-eV plasma, the corresponding electron density is  $N_e = 7.9 \times 10^{20} \text{ cm}^{-3}$ .

Figures 1(a)–1(c) show partial cross sections as functions of total angular momentum  $L$  (which for  $s \rightarrow s$  or  $s \rightarrow p$  transitions is the same as the initial partial-wave angular momentum  $l$ ). The  $2s$  and  $2p$  atomic states are taken to be degenerate. Comparing the partial cross sections in Figs. 1(a)–1(c), one confirms that the BI results slowly approach the three-state close-coupling (3 CC) results for optically allowed transitions ( $s \rightarrow p$ ) at large  $L$ , where both distortion and strong-coupling effects are small. The agreement is even better at higher energies (not shown). The DWII and two-state close-coupling (2 CC) results are

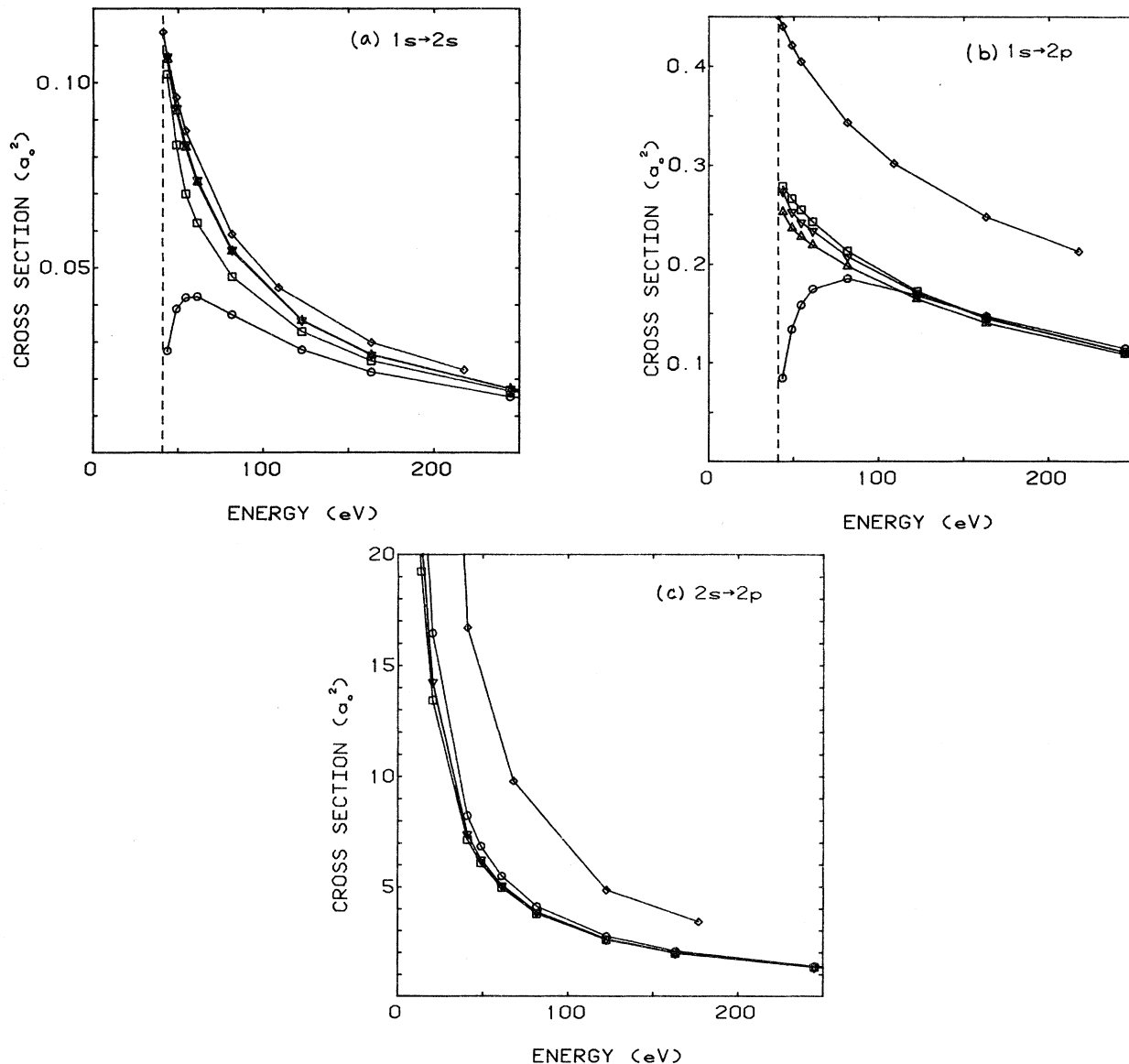


FIG. 2. Excitation cross sections vs energy for  $e\text{-He}^+$  scattering. Plasma represented by Debye-Hückel model with  $\Lambda = 10a_0$  ( $5.9 \text{ \AA}$ ).  $\square$  (3 CC);  $\triangle$  (2 CC);  $\nabla$  (DWII);  $\circ$  (BI);  $\diamond$  (CBI). (a)  $1s$  to  $2s$  cross section. Threshold energy = 40.8 eV. (b)  $1s$  to  $2p$  cross section. Threshold energy = 40.8 eV. (c)  $2s$  to  $2p$  cross section. Threshold energy = 0.0 eV. (3 CC and 2 CC results are the same.)

very similar, indicating that the coupling is relatively weak. Coupling all three states together (3 CC) affects the  $1s \rightarrow 2s$  and  $1s \rightarrow 2p$  cross sections; but the  $2s \rightarrow 2p$  cross section is essentially unchanged. Comparison of the 2 CC and 3 CC results for  $1s \rightarrow 2s$  and  $1s \rightarrow 2p$  transitions shows that for small  $L$  there is some redistribution of flux from the  $2s$  into the  $2p$  state. This situation is reversed at larger  $L$  as the long-range, direct  $1s \rightarrow 2p$  coupling effectively increases the range of the electron-ion interaction contributing (indirectly) to the  $1s \rightarrow 2s$  transition.

To reduce computation time for the  $2s \rightarrow 2p$  transition, where the long-range coupling is particularly strong, we have calculated CC and DWII partial cross sections only for small values of  $L$ . For larger  $L$  ( $L \geq 12$ , for this ener-

gy), where BI results are within 3% of CC, only BI cross sections were calculated; and the total cross section is given to a good approximation by

$$Q \cong Q^{\text{BI}} + \sum_{L=0}^{L'} (Q_L^{\text{CC}} - Q_L^{\text{BI}}), \quad (7)$$

where  $Q^{\text{BI}}$  is the total BI cross section; and  $Q_L^{\text{CC}}$  and  $Q_L^{\text{BI}}$  are the partial cross sections for the CC and BI approximations, respectively.

In Figs. 2(a)–2(c) total excitation cross sections are displayed as functions of the energy for the plasma conditions described above. For comparison, unscreened CBI results are also shown.<sup>19</sup> For the optically allowed  $1s \rightarrow 2p$

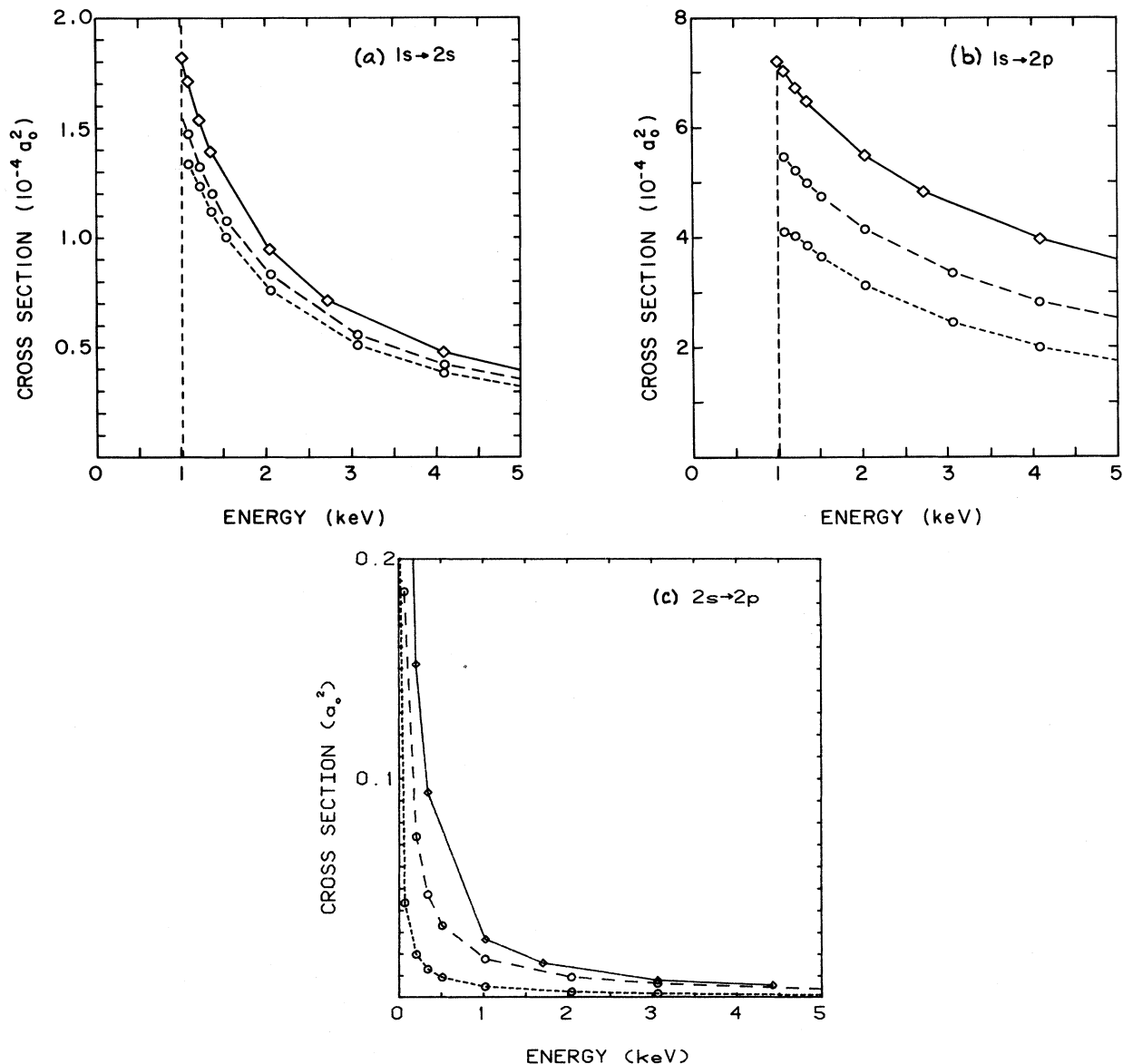


FIG. 3. Excitation cross sections (3 CC) vs energy for  $e\text{-Ne}^{9+}$  scattering for plasma conditions  $N_e = 1.1 \times 10^{24} \text{ cm}^{-3}$ ,  $T = 500 \text{ eV}$  ( $\Lambda = 3a_0$ ,  $R_s = 2.4a_0$ ), and various plasma models. Solid line (CBI); dashed line (Debye-Hückel); dotted line (ion sphere). (a)  $1s$  to  $2s$  cross section. Threshold energy = 1.02 keV. (b)  $1s$  to  $2p$  cross section. Threshold energy = 1.02 keV. (c)  $2s$  to  $2p$  cross section. Threshold energy = 0.0 eV.

and  $2s \rightarrow 2p$  transitions, the presence of the plasma significantly reduces the total cross section at all energies. This is expected, since the long-range ( $r^{-2}$ ) coupling matrix element should be particularly sensitive to screening. Except near threshold, the cross sections are relatively insensitive to the scattering approximation employed; even BI gives good results for energies above 122 eV (three times the  $1s \rightarrow 2p$  threshold), and DWII is quite accurate at all energies. This behavior parallels that of the unscreened bare-ion results, where the  $1s \rightarrow 2p$  cross section shows little variation with respect to the choice of scattering approximation.<sup>20</sup>

The situation is very different for the optically forbid-

den  $1s \rightarrow 2s$  transition. The presence of a plasma, as modeled here, does not appreciably reduce the cross section, since the coupling is intrinsically short range (exponential) even in the absence of plasma screening. However, as in the bare-ion case,<sup>20</sup> the  $1s \rightarrow 2s$  cross section is expected to be very sensitive to details of the collision dynamics (viz., exchange and correlation effects). The BI approximation is poor except at very high energies ( $E \gtrsim 250$  eV). Finally, including coupling with the  $2p$  state reduces somewhat the  $1s \rightarrow 2s$  cross section.

### B. Plasma-screening effects

In order to illustrate differences in the cross sections corresponding to fixed plasma conditions but different screening models, we show in Figs. 3(a)–3(c) several 3 CC results for the  $1s \rightarrow 2s$ ,  $1s \rightarrow 2p$ , and  $2s \rightarrow 2p$  transitions in  $\text{Ne}^{9+}$ . Cross sections are shown for the Debye-Hückel and ion-sphere models. The CBI results<sup>18,19</sup> for unscreened  $\text{Ne}^{9+}$  are also given for comparison.

For both model potentials, the (forbidden)  $1s \rightarrow 2s$  cross sections display little sensitivity to the plasma screening. In contrast, the (allowed)  $s \rightarrow p$  cross sections are reduced considerably with respect to the CBI values. (This trend continues as the screening is made stronger.) For a given set of plasma conditions, the ion-sphere model represents by far the stronger screening, the corresponding reductions in cross section being roughly twice those of the Debye-Hückel model. In addition, narrow resonances (not shown) appear very near threshold for the ion-sphere potential. These are simply potential resonances occurring in the  $l=1$  or  $2$  final-state partial waves, due to centrifugal barriers outside the strongly attractive, but very short-range ion-sphere interaction. (Resonances should also occur in the Debye-Hückel model, but they should be narrower and lie even closer to threshold.)

### C. Target-state effects

We have also investigated the effect of varying the nuclear charge  $Z$ . Since in the scattering equations the quantities  $E$ ,  $Q$ ,  $R_z$ , and  $\Lambda$  scale approximately as  $E/Z^2$ ,  $Z^4Q$ ,  $ZR_z$ , and  $Z\Lambda$ , respectively, we plot in Figs. 4 and 5 scaled 3 CC cross sections versus scaled energy for  $\text{He}^+$ ,  $\text{Ne}^{9+}$ , and  $\text{Ar}^{17+}$ ;  $Z\Lambda$  and  $ZR_z$  are held constant. The BI cross sections scale exactly, but the presence of the nuclear term in the "distortion" potential causes departure from exact scaling for CBI. Similarly, the 3 CC cross sections do not scale exactly. However, an approximate scaling law does hold. With respect to *scaled* quantities, one can say that at a fixed value of the scaled screening length, plasma-screening effects decrease slightly as  $Z$  increases. Just above threshold, where the cross sections are influenced by resonances, the scaling can fail completely.

Finally, we investigated the effect of removing the  $2s \rightarrow 2p$  degeneracy. We calculated 3 CC cross sections for  $\text{Ne}^{9+}$  in the Debye-Hückel screening model with  $\Lambda = 3a_0$ , first using the fine-structure splitting ( $\Delta E = 0.416$  eV),<sup>21</sup> and then using energy eigenvalues calculated for an atom in a Debye potential ( $\Delta E = 1.22$  eV).<sup>21</sup> The  $1s \rightarrow 2s$  and  $1s \rightarrow 2p$  cross sections were unaffected. The  $2s \rightarrow 2p$  cross section was changed only slightly: At low energies (e.g.,

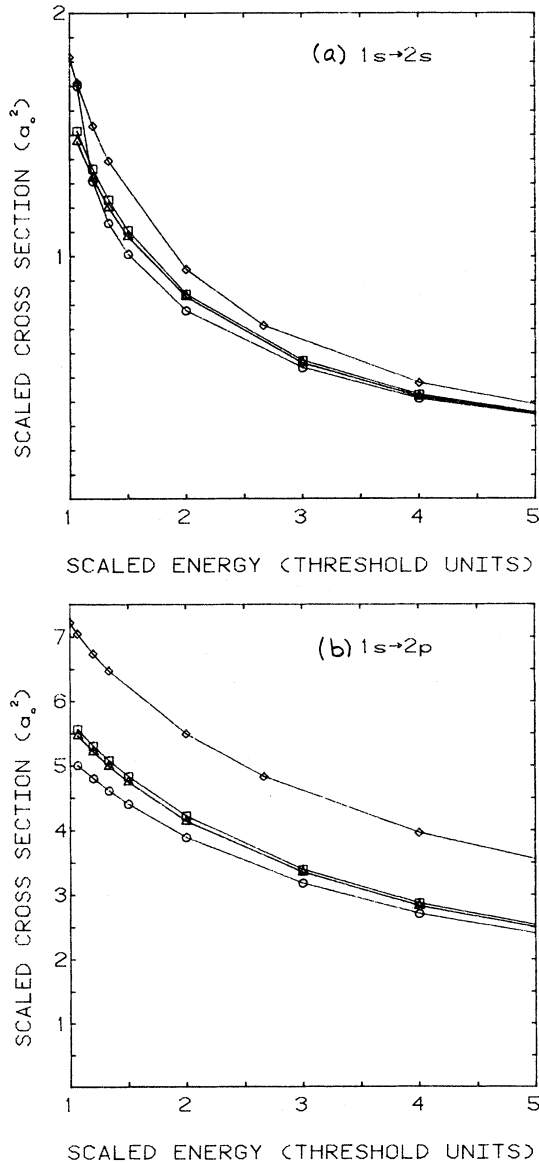


FIG. 4. Scaled excitation cross section ( $Z^4Q$ ) vs scaled energy ( $E/Z^2$ ). Plasma represented by Debye-Hückel model with  $Z\Lambda = 30a_0$ .  $\diamond$ —CBI ( $Z = \infty$ ,  $\Lambda = \infty$ );  $\square$ — $\text{Ar}^{17+}$  ( $Z = 18$ ,  $\Lambda = 1.67a_0$ );  $\triangle$ — $\text{Ne}^{9+}$  ( $Z = 10$ ,  $\Lambda = 3a_0$ );  $\circ$ — $\text{He}^+$  ( $Z = 2$ ,  $\Lambda = 15a_0$ ). (a)  $1s$  to  $2s$  cross section. (b)  $1s$  to  $2p$  cross section.

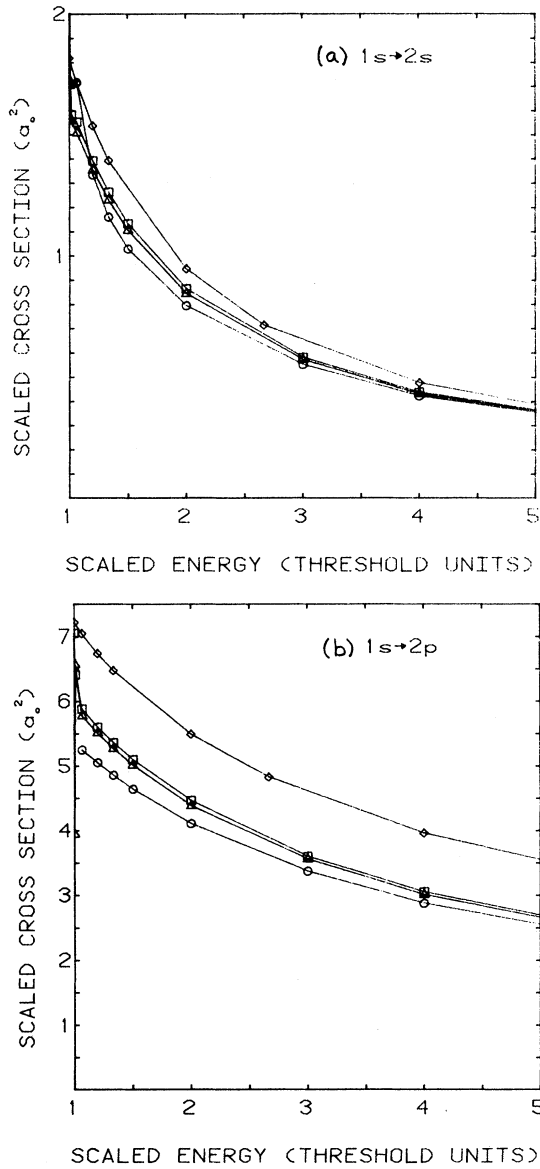


FIG. 5. Scaled excitation cross section ( $Z^4Q$ ) vs scaled energy ( $E/Z^2$ )—plasma represented by ion-sphere model with  $ZR_z = 60a_0$ .  $\diamond$ —CBI ( $Z = \infty$ ,  $R_z = \infty$ );  $\square$ —Ar<sup>17+</sup> ( $Z = 18$ ,  $R_z = 3.33a_0$ );  $\triangle$ —Ne<sup>9+</sup> ( $Z = 10$ ,  $R_z = 6a_0$ );  $\circ$ —He<sup>+</sup> ( $Z = 2$ ,  $R_z = 30a_0$ ). (a)  $1s$  to  $2s$  cross section. (b)  $1s$  to  $2p$  cross section.

68 eV), the cross sections were reduced by about 10% for the larger splitting; at higher energies the differences were found to fall rapidly, becoming less than 1% at 1.02 keV.

## V. DISCUSSION

It is not surprising to find that optically allowed transitions respond very differently than optically forbidden ones to the plasma environment, due to the different ranges of coupling interaction. In our model, in which the target states are not Stark mixed, forbidden transitions (especially  $s \rightarrow s$ ) are more sensitive to details of the collision dynamics than to plasma screening and, for such

transitions, it might suffice to ignore plasma effects completely and simply adopt the best bare-ion results available. For optically allowed transitions, though, the situation is reversed. Here a distorted-wave or, at higher energies, even a plane-wave Born calculation gives reasonably good agreement with close-coupling results provided that screened interactions are used. We can suggest one possible prescription for improving upon these simpler calculations: Detailed studies of the partial cross sections for various Debye screening lengths have shown that high- $L$  partial waves are more significantly affected by the plasma than the more penetrating small- $L$  waves. Also, exchange and short-range correlation effects are expected to be more significant at small  $L$ . Thus it seems reasonable to combine higher- $L$  (say  $L \geq 2$ ) screened partial cross sections with the lower- $L$  results of a more careful bare-ion calculation,<sup>22</sup> thereby obtaining a fairly accurate "hybrid" total excitation cross section.

We did not construct any such hybrid cross sections, but, in connection with the partial wave calculations, we did investigate another even simpler prescription for approximating detailed cross section results. The standard treatment of elastic Coulomb scattering in a plasma limits the Rutherford cross section by imposing a cutoff at large impact parameters (i.e., small angles),  $\rho_{\max} \simeq \Lambda$ , the Debye length; in the quantal picture this corresponds to a cutoff in partial waves at  $L_{\max} \simeq k\Lambda$ . This suggests an approximation whereby, in lieu of performing calculations involving screened potentials, one merely truncates the partial wave summation, Eq. (5), of unscreened cross sections at  $L = L_{\max}$ . Test calculations suggest that this scheme can greatly underestimate the effect of plasma screening on allowed transitions.

In addition we have found, as one might expect, that at a given value of  $\Gamma$  the ion-sphere model results in greater reductions in the cross sections than does the Debye-Hückel model, which represents a less severe screening of the electron-ion interaction. We anticipate that cross sections determined from a more elaborate static potential, such as that of Dharma-Wardana and Taylor<sup>4</sup> or of Gupta and Rajagopal,<sup>5</sup> will lie between our Debye-Hückel and ion-sphere results. In fact, in their scattering calculations Davis and Blaha<sup>23</sup> employed the potential of Ref. 4, but at  $\Gamma \approx 1$  it is little different from a Debye-Hückel potential (cf. their Fig. 1). However, in the limit of no screening, their results disagree with both Coulomb-Born<sup>22</sup> and plane-wave Born<sup>7</sup> calculations; we do not understand this discrepancy.

We showed in Sec. IV that scaled cross sections ( $Z^4Q$ ) increase only slightly with  $Z$  at a fixed value of the scaled screening length. The scaled screening lengths themselves behave as

$$ZR_z \propto \left[ \frac{Z^2}{T} \right] \left[ \frac{1}{\Gamma} \right] \quad \text{and} \quad Z\Lambda \propto \left[ \frac{T}{Z^2} \right]^{1/2} \left[ \frac{1}{\Gamma} \right]^{3/2}. \quad (8)$$

(We have ignored the difference between  $Z$  and  $Z - 1$ .) Because the ionic species that are most abundant in a plasma are those for which  $T/Z^2 \sim \text{const}$ ,<sup>24</sup> for equivalent plasma conditions (fixed  $\Gamma$ ), the scaled cross sections will vary only weakly with  $Z$ .

Several improvements in these calculations suggest themselves. First, we have ignored dynamic screening effects entirely. This is particularly important in the description of the interaction between the bound and projectile electrons, which is responsible for inelastic transitions. To the extent that a spherical potential (which does not mix  $l$  states) is valid, the *static*, spherically symmetric screening used here maximizes the effect of the plasma environment. Another complication for the development of a dynamic screening model arises from the suprathermal electrons that exist in laser-heated matter. These fast, non-Maxwellian particles can partially screen electrons that have energies a few times  $kT$  (and therefore are most important for H-like ion resonance excitations). Second, refinements could be made in the description of the scattering dynamics. In particular, allowing for resonances might increase the cross sections. However, continuum lowering will change the resonance structure considerably, and sharp cross section features will be washed out by fluctuations in the plasma.

Finally, we have neglected all effects of neighboring plasma ions on individual electron-ion scattering events. The major influence of plasma ions is to produce a quasi-static electric microfield whose average strength can be quite large. It seems likely that, at energies well above threshold, the Stark mixing of nearly degenerate target

states will have a larger effect on cross sections than any modification of the free-electron's trajectory: The size of the former can be surmised from the large differences in  $1s-2s$  and  $1s-2p$  cross sections computed for unmixed  $2s$  and  $2p$  states (cf. the Born calculations in Ref. 7 and Sec. IV A of this paper), while that of the latter can be estimated from differences—for a given transition—between Coulomb-Born cross sections<sup>21</sup> and plane-wave Born cross sections for infinite screening lengths.<sup>7</sup>

#### ACKNOWLEDGMENTS

The authors are grateful to Professor M. A. Morrison and Dr. A. N. Feldt of the University of Oklahoma for providing the coupled-channels computer program, and to Dr. G. J. Hatton of Rice University for assistance with the Born calculations. B. L. W. would like to thank Dr. C. B. Tarter of the Theoretical Physics Division of Lawrence Livermore National Laboratory for hospitality and generous provision of computer time. This work was supported in part (B. L. W. and N. F. L.) by the U.S. Department of Energy, Office of Basic Energy Sciences and by The Robert A. Welch Foundation. J. C. W. was supported by the Department of Energy Contract No. DE-AC02-76-CHO-3073.

\*Present address: Lawrence Livermore National Laboratory, Livermore, Calif. 94550.

<sup>1</sup>G. Bekefi, C. Deutsch, and B. Yaakobi, in *Principles of Laser Plasmas*, edited by G. Bekefi (Wiley, New York, 1976).

<sup>2</sup>V. A. Boiko, S. A. Pikuz, and A. Ya Faenov, *J. Phys. B* **12**, 1889 (1979).

<sup>3</sup>J. C. Weisheit, in *Applied Atomic Collision Physics*, edited by H. S. W. Massey (Academic, New York, to be published), Vol. II.

<sup>4</sup>M. C. W. Dharma-wardana and R. Taylor, *J. Phys. C* **14**, 629 (1981).

<sup>5</sup>U. Gupta and A. K. Rajagopal, *Phys. Rep.* **87**, 260 (1982).

<sup>6</sup>The current status of this subject is described in *J. Quant. Spectrosc. Radiat. Transfer* **27**, (3) (1982).

<sup>7</sup>G. J. Hatton, N. F. Lane, and J. C. Weisheit, *J. Phys. B* **14**, 4879 (1981).

<sup>8</sup>D. Clayton, *Principles of Stellar Evolution and Nuclear Synthesis* (McGraw-Hill, New York, 1968).

<sup>9</sup>J. C. Stewart and K. D. Pyatt, *Astrophys. J.* **144**, 1203 (1966).

<sup>10</sup>B. F. Rozsnyai, *J. Quant. Spectrosc. Radiat. Transfer* **22**, 337 (1979).

<sup>11</sup>N. A. Krall and A. W. Trivelpiece, *Principles of Plasma Physics* (McGraw Hill, New York, 1973).

<sup>12</sup>B. Yaakobi, D. Steel, E. Thorsos, A. Hauer, B. Perry, S. Skupsky, J. Geiger, C. M. Lee, S. Letzring, J. Rizzo, T. Mukaiyama, E. Lazarus, G. Halpern, H. Deckman, J. Delettretz, J. Soures, and F. McCrory, *Phys. Rev. A* **19**, 1247 (1979).

<sup>13</sup>B. Yaakobi, S. Skupsky, R. L. McCrory, C. F. Hooper, H.

Deckman, P. Bourke, and J. Soures, *Phys. Rev. Lett.* **44**, 1072 (1980).

<sup>14</sup>M. J. Seaton, *Proc. Phys. Soc. London* **77**, 174 (1961).

<sup>15</sup>P. G. Burke and K. Smith, *Rev. Mod. Phys.* **34**, 458 (1962); I. C. Percival and M. J. Seaton, *Proc. Cambridge Philos. Soc.* **53**, 654 (1957).

<sup>16</sup>S. Volonte, *J. Phys. D* **11**, 1615 (1978).

<sup>17</sup>W. M. Sams and D. J. Kouri, *J. Chem. Phys.* **51**, 4809 (1969); M. A. Morrison, in *Electron-Molecule and Photon Molecule Collisions*, edited by T. N. Rescigno, V. McKoy, and B. Schneider (Plenum, New York, 1979).

<sup>18</sup>A. Burgess, D. G. Hummer, and J. A. Tully, *Philos. Trans. R. Soc. London* **266**, 225 (1970).

<sup>19</sup>The Coulomb-Born I cross sections are included here and elsewhere in the paper to provide a rough upper limit to the bare-ion cross sections. For consistency, the  $Z \rightarrow \infty$  cross sections are used in all cases (see Ref. 18 for discussion of the fact that in this limit the CBI and CBII approximations are identical).

<sup>20</sup>R. J. W. Henry, *Phys. Rep.* **68**, 1 (1981).

<sup>21</sup>F. J. Rogers, H. C. Graboske, Jr., and D. J. Harwood, *Phys. Rev. A* **1**, 1577 (1970).

<sup>22</sup>S. A. Wakid and J. Callaway, *J. Phys. B* **13**, L605 (1980).

<sup>23</sup>J. Davis and M. Blaha, in *Physics of Electronic and Atomic Collisions*, edited S. Datz (North-Holland, Amsterdam, 1982), p. 811.

<sup>24</sup>D. E. Post, R. V. Jensen, C. B. Tarter, W. H. Grasberger, and W. A. Lokke, *At. Data Nucl. Data Tables* **20**, 397 (1977).